International Journal of the Korean Society of Precision Engineering, Vol. 1, No. 1, June 2000.

Study on the Reconstruction of Skull Prototype using CT image and Laser Scanner

Sung-Min Hur* and Seok-Hee Lee**

*Dept. of Mechanical and Intelligent Systems Engineering, Pusan National University

**School of Mechanical Engineering, Pusan National University

ABSTRACT

The importance of shape reconstruction is increasing in many areas such as RPD (Rapid Product Development) and reverse engineering. Typical data in these areas are mainly classified as the shape data measured by a laser scanner and the data extracted from the CT image.

The goal of this research is to realize three-dimensional shape construction by showing a possible way to analyze input image data and reconstruct the original shape. Two main steps of the reconstructing process are obtaining cross-section data from image processing and linking loops between one slice and the next. Objects reconstructed in this way are compared with other objects using a laser scanner and modelled by commercially available software. The technique is expected to be used in reverse engineering applications and the object modeling with automated process.

Key Words: Reverse engineering, sliced image data, laser scanner, CT, RP, STL

1. Introduction

One of the distinct progress in current production and design processes is to employ the technology of three dimensional reconstruction using data measured on an existing physical shape. This technique is referred to as reverse engineering and enables reproduction of objects without CAD data. Reverse engineering is also useful for prototype shapes that are difficult to model directly with three-dimensional CAD software. The physical prototype models, wood patterns and clay models were built and then measured using computer tomography (CT), magnetic resonance imaging (MRI), laser scanner, or coordinate measuring machine (CMM), as appropriate(1,2).

Yancey(3) addressed a method on the 3 dimensional reconstruction of an object from CT image data, and Kristoff(4) studied the conversion of MRI data to CAD data for the development of medical devices.

Miyake(5) proposed an algorithm to reconstruct 3dimensional surface from positional slice data.

Ueng(6) used surface fitting algorithm to get sweep surface for 3 dimensional reconstruction from measured coordinate data and Bajaj(7) implemented 3 dimensional reconstruction from planar cross section with use of triangulation algorithm.

The purpose of this paper is to present algorithms used to construct a prototype of an ancient skull. The data sources are two different images; CT image data, which describes a 2 dimensional cross-section of the scan, and laser scanner data. Two approaches are evaluated based on manufacturability, cost, accuracy, surface finish, and other factors.

2. IMAGE PROCESSING

In order to extract the needed information from each CT image data slice, image processing is required to improve the image as much as possible. This information includes the number of slices, the number of loops composing a slice, the number of vertices on a loop, and coordinates of each vertex. This is accomplished by combining four sequential processes: binary image processing, morphology processing, boundary detection, and thinning processing.

2.1 Binary image processing

Binary image processing segments the output intensity of each pixel by comparing the input intensity value of each pixel with the provided threshold value. Binary image processing is performed based on the equation (1) and its result is shown in Fig. 1.

$$g(x,y) = \begin{pmatrix} 1 & f(x,y) \geq t \\ 0 & f(x,y) < t \end{pmatrix} \quad (1)$$

$f(x,y)$: intensity of pixel before binary process
$g(x,y)$: intensity of pixel after binary process
t : threshold value

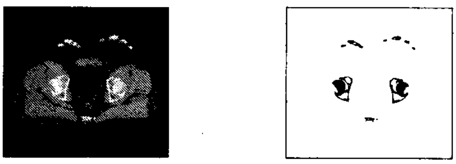

(a) CT image (b)Binary image

Fig. 1 Binary process

2.2 Morphology process

Some regions that are not closed may exist after binary image processing. Since the boundary profile extracted from these regions is distorted, the closing process should be required to deal with this problem. Erosion operation can reduce the size of the object with respect to the background, and is usually applied to eliminate image noise as defined in equation(2). Dilation plays a contrary role compared to erosion, and is defined in equation(3). The closing operation of an image is defined in equation (4) and performed as shown in Fig. 2.

$$A \oplus B = \bigcup_{b \in B} A_b \quad (2)$$

$$A \ominus B = \bigcap_{b \in B} A_{-b} \quad (3)$$

$$B \cdot K = (B \oplus K) \ominus K \quad (4)$$

where A, B and K are the structure elements.

(a) CT Image (b) Closing

Fig. 2 Closing of CT image

2.3 Boundary detection

Prewitt mask is employed for the boundary detection. The gradient magnitude of prewitt operator, M, can be obtained from equation (5).

In equation (5), variables A0~A7 are factors of mask, and if value c equals 1, the mask becomes a prewitt mask(see Fig. 3) where a clear edge can be extracted(8) as shown in Fig. 4.

1	1	1	-1	0	1	a_0	a_1	a_2
0	0	0	-1	0	1	a_7	[i,j]	a_3
-1	-1	-1	-1	0	1	a_6	a_5	a_4

Fig. 3 Prewitt mask

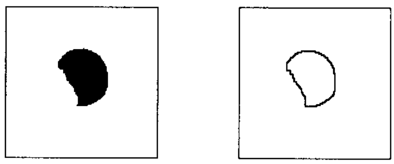

(a) Closed image (b) Detected edge

Fig. 4 Edge detection

2.4 Thinning process

Thinning is a process to generate the same thickness boundary with 1 pixel thickness from the unstructured line, so that clearer images can be obtained(8) as shown in Fig. 5.

(a) Image with detected edge (b)Thinned image

Fig. 5 Thinning process

2.5 Information on sliced image data

The vertex composing the detected boundary is obtained by searching those connected points in the counter-clockwise sequence from the leftmost edge of the pixel as shown in Fig. 6 and the repeated search result is illustrated in Fig. 7. The next step is to eliminate vertex within preallocated tolerance to avoid unnecessary operation time as illustrated in Fig. 8.

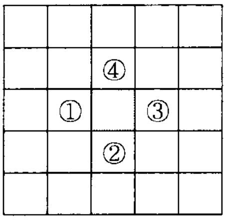

Fig. 6 Sequence to find point

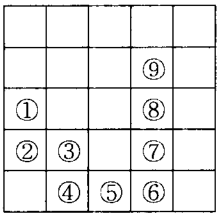

Fig. 7 Connected points

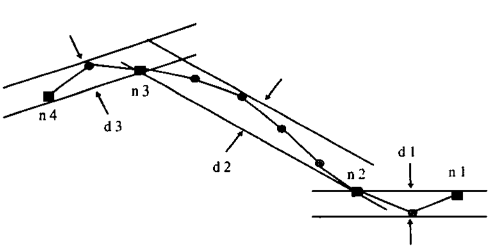

Fig. 8 Elimination of vertex

3. STL PROCESS

Slice list is constructed based on slice data containing information on slice number, loop starting point, vertex coordinates, and loop ending point. As shown in Fig. 9, the total image is composed of many slices, each slice consists of many loops, and each loop includes a set of vertexes.

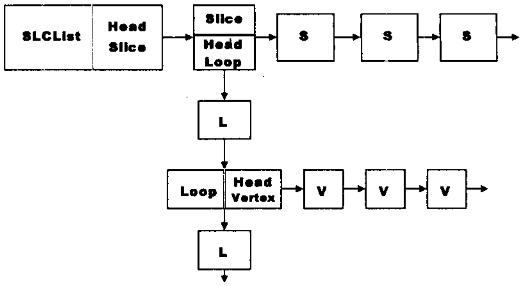

Fig. 9 SLCList structure

3.1 Classification of loop

The intersection between two loops projected to a 2D plane should be investigated to establish the relation between the loops in each slice. The relations between loops are classified into three categories as shown in Fig. 10.

Fig. 10 (a) illustrates the inclusion between loops on a slice in the branching area and Fig. 10 (b) shows that there are no intersections between loops in a slice and the next slice in the capping area. Fig. 10 (c) shows that there is intersection between loops in a slice and the next one on the branching area.

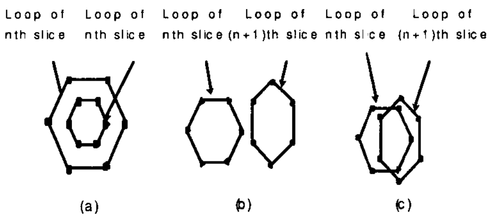

Fig. 10 Classification of loop state

3.2 Triangulation process

Triangulation process can be classified in two types according to its position, one is within one layer and the other is between layers. First, the loop in capping area should be a polygon itself, so it can be triangulated in general method(9) as shown in Fig. 11. Second case includes the triangulation between loops in Fig. 12.

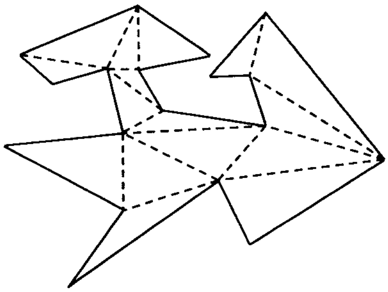

Fig. 11 Triangulation of polygon

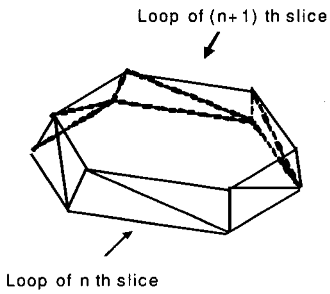

Fig. 12 Triangulation between different Slices

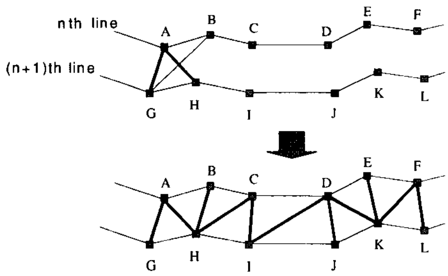

Fig. 13 Christiansen algorithm

As illustrated in Fig. 13, the Christiansen algorithm(5) is used for efficient triangulation, where a vertex on a current loop connects to the closest vertex on the next loop. The triangular patch represents the basic element of a surface. A surface is generated by defining segments between slices and connecting them.

In Fig. 10 (a), an interior loop forms a pair with the only interior loop on the next slice during triangulation. An exterior loop is processed in the same way as an interior loop. In Fig. 10 (b), the polygon comprising each loop is triangulated individually(9). In Fig. 10 (c), the Christiansen algorithm is employed in the case of only one loop-to-one loop correlation. However, in the case of one loop-to-many loop correlation, the loops of a slice should be put together by using bridge edges with following process in Figs. 14~16 so that the triangulation can maintain slice connectivity.

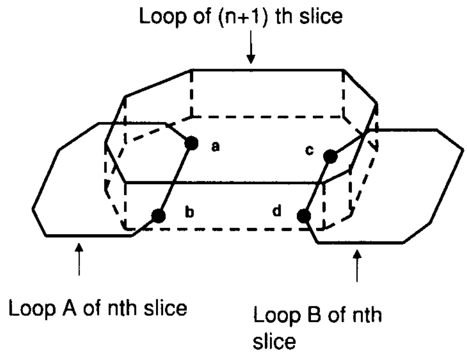

Fig. 14 Case of 1 : m triangulation

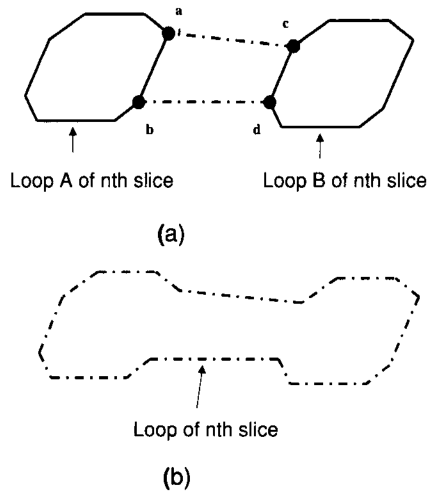

Fig. 15 Connection of two loops

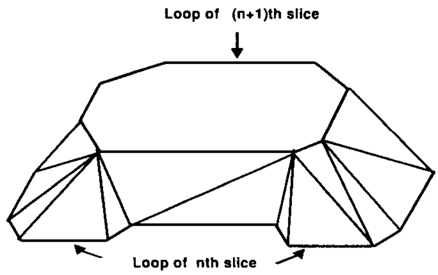

Fig. 16 Result of 1 : m triangulation

4. RESULTS AND DISCUSSION

As shown in Fig. 17, two different skulls were fabricated based on two different measured data; CT image data and laser scanned data, and compared with respect to manufacturability, cost, and accuracy.

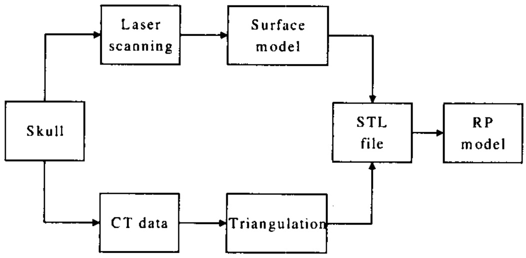

Fig. 17 Comparison of two ways to build skull

4.1 Skull model reconstruction using CT data

Fig. 18 shows the first skull model used in this research. The CT image data was sliced at 3mm interval. The CT image data in Fig. 19 changed into gray image at the 256 intensity level. Figs. 20 (a)~(d) show the results of image processing, consisting of the binary process, morphology, edge detection, and thinning process. Fig. 21 shows the STL model with the triangulation of each sliced image data, and a skull model built by rapid prototyping is illustrated in Fig. 22.

4.2 Skull model reconstruction from laser scanned data

Fig. 23 shows the second skull model which is measured by a laser scanner(Fig. 24). In Figs. 25 and 26, the laser scanned data was visualized and the 3D surface model was constructed respectively. The manufactured skull model is shown in Fig. 27.

Fig. 18 Skull I

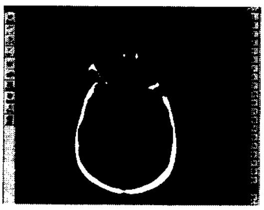

Fig. 19 Original CT data

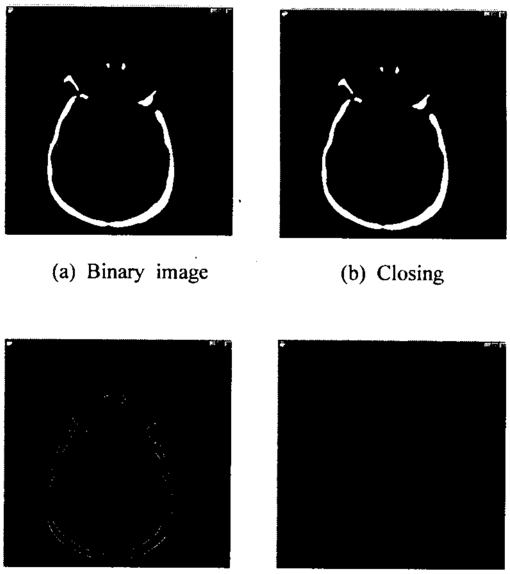

(a) Binary image (b) Closing

(c) Prewitt masking (d) Thinning

Fig. 20 Image processing

Fig. 21 STL model

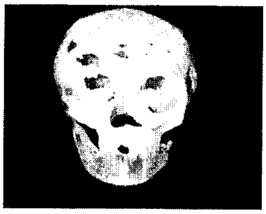

Fig. 22 RP model

Fig. 23 Skull II

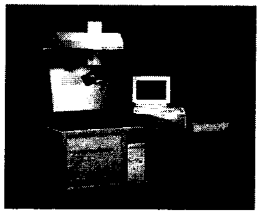

Fig. 24 Laser scanner

Fig. 25 Scan data

Fig. 26 Surface model

Fig. 27 RP model

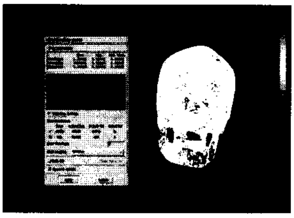

Fig. 28 Comparison of error

4.3 Comparison of manufactured models

Fig. 28 shows the comparison between the laser scan data of skull model 2 and its outer surface STL file constructed from CT image data. Average 0.9mm error resulted from the resolution in image processing.

The approach to build skull models by laser scan data has the following problems. It is impossible to model the feature inside because of no laser penetration. This approach increases cost due to large amount of resin and laser power to be used. In addition, it is difficult to define the features near the balls which are used for registration during the scanning process.

In contrast, the approach to build skull models by CT image data has following characteristics. Cost can be saved during the RP process due to the possibility of inside modeling. Overall surface finish can be deteriorated because of its optimal orientation to build the fragile part of the mouth area. Many sharp vertices and supports built inside the model also pose serious problems during the RP process and postprocess. Special care must be taken by the operator where sharp vertices exist to avoid breakdown during the RP process.

5. Conclusion

In this research, two steps were considered to construct a 3D object with STL format from 2D CT slicing data. The first step is image processing for obtaining preliminary data for STL construction, which is composed of the binary process, morphology, boundary detection, and thinning process. The second step includes the construction of a slice list structure, establishment of correlation between loops, triangulation between loops, and output in STL format. Two skull models are made by using different data; CT image data and laser scanned data. Comparison with respect to manufacturability, cost, and accuracy shows that the CT image data approach provides certain reasonable benefits. The manufactured model in this process can be applied not only to the reconstruction of ancient skulls but can also be substituted for valuables which are difficult to release to the public due to the danger of breakdown and storage.

References

1. Kathryn A. Ingle, "Reverse Engineering", McGraw-Hill Inc., 1994
2. Yasser Hosni, Labiche Ferreira, Ramesh Burjanroppa, "Rapid Prototyping through Reverse Engineering," 2nd Industrial Engineering Research Conference Proceedings, pp. 420~424, 1993.
3. Robert N. Yancey, Dennis S. Eliasen, S. Trent Neel, James H. Stanley, "Reverse Engineering using Computed Tomography", Proceedings of the Fifth International Conference on Rapid Prototyping, Dayton, Ohio, pp. 141~149, 1994
4. Kristoff J., "Mapping Human Anatomy from MRI Data for Improved Product Development", MD&DI, 1997, http://www.devicelink.com/mddi/archive/97/03/017.html
5. Y. Miyake, T. Kondo, S. Kaneko, S. Igarashhi, H. Narahara, "Reconstruction of Three Dimensional Surface from Slice Positional Data", Chapman& Hall, 1997
6. Wen-Der Ueng, Jiing-Yih Lai, and Ji-Liang Doong, "Sweep surface reconstruction from three dimensional measured data", Computer Aided Design, Vol. 30, No. 10, 1998, pp. 791~805
7. Chandrajit L. Bajaj, Edward J. Coyle and KwunNan Lin, "Arbitrary Topology Shape Reconstruction from Planar Cross Sections", Graphical models and Image processing, Vol. 58, No. 6, 1996, pp. 524~543
8. Ramesh Jain, Rangachar Kasturi, Brian G. Schunck, "Machine Vision," McGraw-Hill Inc., 1995.
9. Joseph O'Rourke, "Computational Geometry in C", Cambridge University Press, 1994.